Nucleic Acids Research, 1996, Vol. 24, No. 9 **1727–1733**

A 39 amino acid fragment of the cell cycle regulator p21 is sufficient to bind PCNA and partially inhibit DNA replication *in vivo*

Junjie Chen, Richard Peters[1,2], Partha Saha, Patrick Lee, Annie Theodoras[3], Michele Pagano[3], Gerhard Wagner[1] and Anindya Dutta*

Department of Pathology, Division of Molecular Oncology, Brigham and Women's Hospital, Harvard Medical School, 75 Francis Street, Boston, MA 02115, USA; [1]Department of Biological Chemistry and Molecular Pharmacology, Harvard Medical School, 240 Longwood Avenue, Boston, MA 02115, USA; [2]Department of Medicine, Massachusetts General Hospital, Fruit Street, Boston, MA 02114, USA and [3]Mitotix Inc., One Kendall Square, Building 600, Cambridge, MA 02139, USA

Received January 5, 1996; Revised and Accepted March 11, 1996

ABSTRACT

The cell cycle regulator p21 interacts with and inhibits the DNA replication and repair factor proliferating cell nuclear antigen (PCNA). We have defined a 39 amino acid fragment of p21 which is sufficient to bind PCNA with high affinity (K_d 10–20 nM). This peptide can inhibit DNA replication *in vitro* and microinjection of a GST fusion protein containing this domain inhibited S phase *in vivo*. Despite its high affinity for PCNA, the free 39 amino acid peptide does not have a well-defined structure, as judged from circular dichroism and nuclear magnetic resonance measurements, suggesting an induced fit mechanism for the PCNA–p21 interaction. The association of the small peptide with PCNA was thermolabile, suggesting that portions of p21 adjoining the minimal region of contact stabilize the interaction. In addition, a domain containing 67 amino acids from the N-terminus of PCNA was defined as both necessary and sufficient for binding to p21.

INTRODUCTION

Normal cell cycle progression involves a sequential increase in the levels of various cyclins, their association with corresponding cyclin-dependent kinases (cdk) and sequential activation of these kinase activities in the different phases of the cycle. Cyclins, cdk kinases, the cdk inhibitor p21 and the DNA replication factor proliferating cell nuclear antigen (PCNA) have been found to form a quaternary complex in untransformed cells (1–3). Besides associating with and inhibiting cdk2 kinase (4–8), p21 has an additional activity through its interaction with the DNA replication factor PCNA. PCNA is an auxiliary factor for DNA polymerases δ and ε and is essential for DNA replication *in vitro* and *in vivo* (9–15). p21 interacts with PCNA and inhibits its activity (16–21). p21 is transcriptionally induced by the tumor suppressor protein p53, which is itself increased in response to DNA damage, and it has been suggested that the p21 is an important effector of the growth suppressive function of p53 (22).

We and others have reported that the N-terminal 90 amino acids of p21 inhibited cyclin–cdk kinase activity, DNA replication in *Xenopus* egg extracts and cell growth in *p53* null-transformed cancer cell lines (19,23–25). The C-terminal 77 amino acids of p21 interacted with PCNA and inhibited SV40-based DNA replication and *Xenopus* DNA replication. A small chemical based on the structure of p21 which interacts with and inhibits PCNA could be useful for suppressing cell growth or for inhibiting DNA repair after radio- or chemotherapy. We have determined that peptides based on the structure of p21 suppress cell growth when delivered *in vivo* at high concentrations and have measured the K_d of the peptide–PCNA interaction to determine if it was suitable for pharmacology. Despite the high affinity of the peptide–PCNA interaction, circular dochroism and NMR studies show that the free peptide is flexible in structure, suggesting an induced fit mechanism for the peptide–PCNA interaction. We also demonstrate that the N-terminal 67 residues of PCNA are necessary and sufficient for the interaction and that there are multiple potential binding sites for p21 on each PCNA trimer. Taken together these results indicate that while a peptide derived from p21 may itself be unsuitable for targeting the DNA replication and repair apparatus, a synthetic chemical based on the structure of the PCNA-bound peptide could be effective *in vivo*.

MATERIALS AND METHODS

Plasmids

pGST-p21, pGST-p21N and pGST-p21C were generated as described (23). pGST-p21M1 and pGST-p21C2 were generated by PCR with *Pfu* polymerase and cloned into *Bam*HI and *Sal*I sites of pGEX-5X3 (Pharmacia). pETPCNA has been described (26).

Protein expression and purification

Bacterially produced proteins were expressed in *Escherichia coli* BL21. Protein induction, cell lysis and affinity purification with

* To whom correspondence should be addressed

glutathione–agarose beads were as described (27). *In vitro* transcription–translation reactions were as suggested by the manufacturer (Promega).

Synthesis of peptides

A 41 amino acid p21C2 peptide (consisting of the 39 C-terminal amino acids of p21 plus two Lys residues at the C-terminal end required for chemical synthesis) was synthesized at the Harvard Medical School Biopolymer Laboratory using a Millagen/Biosearch 9600 synthesizer. The peptide was purified using C18 reverse phase HPLC.

The sequences of peptides used were:
p21C2:QAEGSPGGPGDSQGRKRRQTSMTDFYHSKRR-LIFSKRKPKK;
CSH262:WNSGFESYGSSSYGGAGGYTQAPGGFGAPAPS-QAEKKSRAR;
CSH119:ADAQHAAPPKKKRKVEDPKDF.

Assays

Affinity chromatography on glutathione beads coated with various GST fusion proteins ('pull-down' assays) was as described (23,27), except that washes were with buffer A7.4 (20 mM Tris–HCl, pH 7.4, 1 mM EDTA, 0.01% NP-40, 10% glycerol, 25 mM NaCl). Unlabeled proteins were detected by immunoblotting with appropriate antibodies and ECL reactions. Proteins produced by *in vitro* transcription–translation were labeled with [^{35}S]methionine and visualized by fluorography.

The SV40 DNA replication reaction was performed as previously described (23,28). Aliquots of 180 ng pSV011 were replicated in a 30 µl reaction containing 100 ng T antigen and 50 µg S100 extract from cell cycle asynchronous 293 cells. Cell extracts and T antigen were pre-incubated on ice for 30 min with GST fusion proteins or peptides without plasmid DNA, then replication reactions were performed by mixing plasmid DNA and incubation at 37°C for 1 h.

Gel filtration

Protein or protein mixtures were incubated on ice for 15 min in A7.4 buffer before loading onto a 25 ml Superose 12 gel filtration column (Pharmacia). Proteins were eluted from the column at a flow rate of 0.4 ml/min. Fractions of 0.5 ml were collected, separated by 15% SDS–PAGE and stained with Coomasie blue to visualize the proteins PCNA (37 kDa), Fen1 (45 kDa) and p21C2 (4.2 kDa).

Scatchard analysis

Bacterially expressed human PCNA was purified as described (26) and labeled with ^{125}I using Bolton–Hunter reagent and following the manufacturer's instructions (Du Pont). Varying amounts of GST–p21C or GST–p21C2 (at least a 30-fold molar excess compared with PCNA) were incubated with a fixed amount of radiolabeled PCNA for 1 h at 4°C or for 15 min at 37°C in buffer A7.4. The GST proteins were recovered by binding to glutathione–agarose beads and the amount of bound PCNA estimated by counting in a gamma counter. All points on the Scatchard plots are the result of at least four different binding assays done on at least two separate days. Care was taken to subtract non-specific binding to GST beads.

The data was analyzed by Scatchard plot according to the equation

$$b/R_t = -b/K_d + B_{max}/K_d$$

where b is the concentration of bound PCNA (in c.p.m./200 µl), R_t is the total concentration of GST fusion protein (in nM), B_{max} is the concentration of total PCNA that can be bound by the GST fusion protein (c.p.m./200 µl) and K_d is the dissociation constant (in nM). K_d was estimated from the slope of the graph of b/R_t versus b (29).

Microinjection

IMR90 human diploid fibroblast monolayers growing on glass coverslips (at 60% density) were synchronized in G0 by serum starvation for 48 h and stimulated to enter G1 by addition of 10% fetal bovine serum. Fifteen hours after re-activation cells in G1 were microinjected with the indicated proteins using an automated microinjection system (AIS; Zeiss). All microinjection experiments were carried out in 3.5 cm Petri dishes containing 3 ml carbonate-free DMEM, in order to avoid a decrease in pH of the medium during the injection. Each cell was injected with protein or peptide (3.75 mg/ml in PBS) together with normal rabbit immunoglobulin (2.5 mg/ml) at a pressure between 50 and 150 hPa. The computer settings for injection were angle '45', speed '10' and time of injection '0.0 s', so as to deliver 0.01–0.05 pl liquid/nucleus. For more details of the microinjection procedure see Pepperkok (30).

DNA synthesis was monitored by incubating with BrdU (100 µM; Amersham) for 10–12 h after microinjection. Coverslips were then rinsed in PBS and fixed for 10 min in –20°C cold methanol/acetone (1:1) and washed again three times with PBS. Microinjected cells were detected by incubation for 1 h with biotinylated horse anti-rabbit IgG (diluted 1:50; Vector Laboratories), washed three times with PBS and incubated with Texas red-conjugated streptavidin (diluted 1:100; Vector Laboratories). Coverslips were subsequently incubated for 10 min with 1.5 M HCl, washed three times with PBS and then incubated for 1 h with a solution of mouse monoclonal anti-BrdU antibody plus nuclease (undiluted; Amersham), followed by a 30 min incubation with a 1:50 dilution of an anti-mouse FITC-conjugated antibody (Vector Laboratories).

All antibody reactions were carried out in a humidified chamber at room temperature and dilutions were made in DMEM containing 10% FCS. Counterstaining for DNA was performed by adding 1 µg/ml bisbenzimide (Hoechst 33258) to the final PBS wash. Immunofluorescence samples were directly mounted in Crystal/mount medium (Biomeda Corp.). Photographs were taken using a Plan-Neofluar 40× lens mounted on a Zeiss Axiophot Photomicroscope and a Color Video Printer Mavigraph on Sony UPC-3010 print paper.

In each experiment ~100 injected cells (and a corresponding number of non-injected cells) were counted. Per cent inhibition of BrdU incorporation was calculated as $[(N - I)/N] \times 100$, where N is percentage BrdU incorporation in non-injected cells and I is percentage BrdU incorporation in cells microinjected with antibodies. The obtained numerical value is independent of possible experimental variations in the number of BrdU-positive cells that had not been injected.

Circular dichroism

Spectra were obtained at a concentration of 22 µM (p21C2) in PBS, pH 7.0. A path length of 0.1 cm in an Aviv 62DS spectropolarimeter equipped with a temperature control unit was used. Spectra were obtained with a scan speed of 1 s at each wavelength. Mean residue

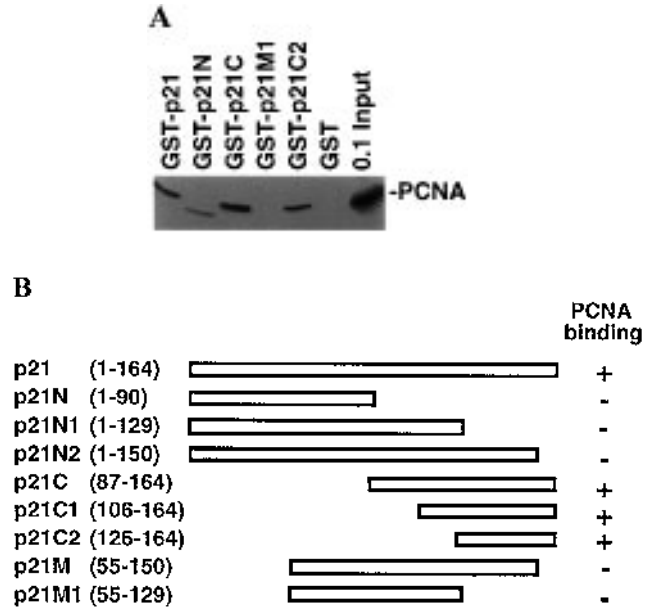

Figure 1. Deletion analysis of p21 shows that the C-terminal 39 amino acids are sufficient for binding PCNA. (**A**) Immunoblot with anti-PCNA antibody. The indicated GST fusion proteins were used to mediate the binding of bacterially produced human PCNA (37 kDa) to glutathione–agarose beads. One tenth of input PCNA is shown for comparison. The smaller band seen in the second lane is the GST–p21N protein, which is ~35 kDa in size. Due to their high protein content, GST fusion proteins produce background bands in the enhanced chemiluminescence reaction used to visualize the immunoblots. (**B**) Schematic summary of deletion derivatives of p21 and their ability to bind PCNA [(A) and data not shown]. The numbers indicate which amino acids of p21 are present in the deletion derivatives.

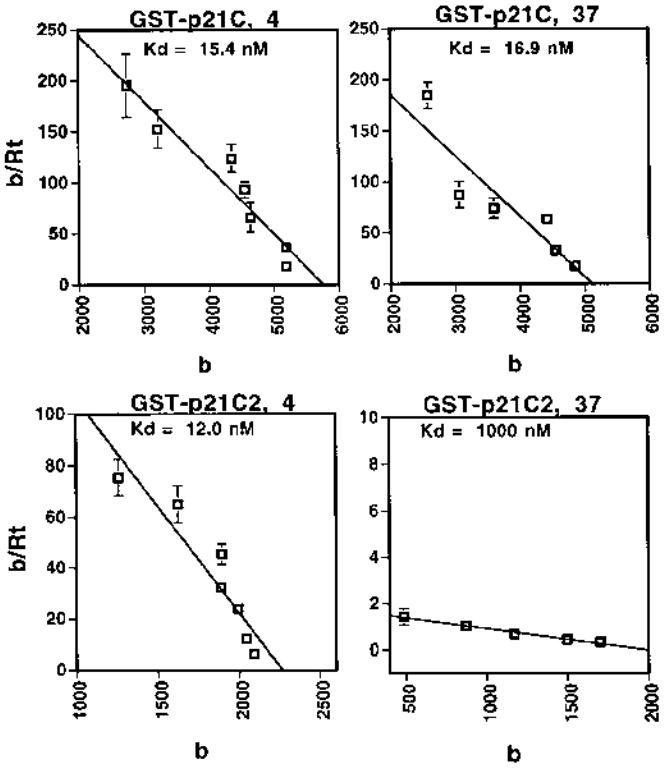

Figure 2. Scatchard analysis of the binding of PCNA to GST–p21C or GST–p21C2 at 4 or 37°C. The *y*-axis shows the ratio of bound PCNA (c.p.m./200 µl) to the total concentration of the GST fusion protein (nM) (b/R_t). The *x*-axis shows the amount of bound PCNA (c.p.m./200 µl) (*b*). Each point is the mean ± SD of four measurements and the slope of the line equals $-1/K_d$.

ellipticity (θ) was calculated with a calculated molecular weight of 4562 g/m.

NMR spectra

All experiments were run on a Varian VXR500 spectrometer. Spectra were recorded at 2 mM sample concentration in PBS, 10% D_2O, pH 7.0. NOESY spectra were recorded at 5 and 25°C with mixing times of 150 and 300 ms. TOCSY spectra were recorded at 25°C with mixing times of 50 and 75 ms.

RESULTS

The C-terminal 39 amino acids of p21 are sufficient to interact with PCNA

Bacterially expressed glutathione S-transferase–p21 (GST–p21), GST–p21C and GST–p21C2 were used as an affinity matrix to demonstrate that PCNA interacts with the last 39 amino acids of p21 (Fig. 1 and data now shown). Scatchard analysis of the interaction (at 4°C) showed that the K_d values for the GST–p21C–PCNA and GST–p21C2–PCNA interactions were 15.4 and 12.0 nM respectively (Fig. 2). At 37°C the K_d of the GST–p21C–PCNA interaction was unchanged, but that of GST–p21C2–PCNA increased 100-fold. A synthetic 41 amino acid peptide corresponding to p21C2 (plus two lysines at the C-terminus) was synthesized. In agreement with the K_d measurements, the synthetic peptide competitively inhibited binding of PCNA to GST–p21 at 4°C (Fig. 3a), but failed to compete with GST–p21 for binding to PCNA at 37°C (Fig. 3b).

These experiments demonstrate that the C-terminal 39 amino acids of p21 are sufficient to bind PCNA. However, an additional 38 amino acids (present in GST–p21C but not in GST–p21C2) stabilize the interaction and prevent loss of affinity as the temperature is increased to the physiological range.

Inhibition of the SV40 replication reaction

Since the interaction of p21 with PCNA inactivates its function as a DNA replication factor, we measured the abilities of the GST fusion proteins to inhibit the SV40-based DNA replication reaction (Fig. 4). The concentration required to obtain 50% inhibition of replication (IC_{50}) was 0.5–1 µM for GST–p21 or GST–p21C and 9 µM for GST–p21C2. The synthetic p21C2 peptide was slightly weaker than GST–p21C2 at inhibiting SV40 replication (IC_{50} 14 µM), but addition of 1% DMSO to the replication reaction improved inhibition by the p21C2 peptide ~2-fold (data not shown). The 10- to 20-fold weaker inhibitory activity of GST–p21C2 compared with GST–p21C could be consistent with its lower affinity for PCNA at 37°C. Inhibition of DNA replication by p21C2 was reversed by addition of excess PCNA (data not shown). We tested whether amino acids 87–125 of p21 (present in p21C, but not in p21C2) contributed to inhibition of SV40 DNA replication by interacting with and inhibiting a second replication factor. A fragment of p21 containing this region, GST–p21M1, was unable to bind PCNA (Fig. 1) or inhibit the DNA replication reaction (Fig. 4). These results suggest that amino acids 87–125 of p21 contribute to replication inhibition only

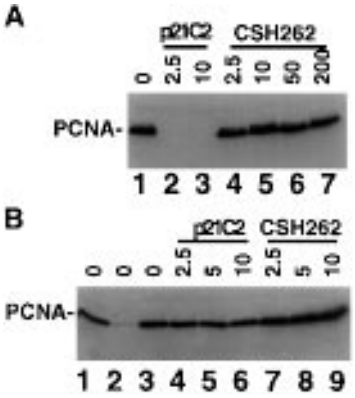

Figure 3. Synthetic p21C2 peptide can competitively inhibit p21–PCNA interaction at 4 but not at 37°C. Binding of PCNA visualized by immunoblotting of bead-bound proteins with anti-PCNA antibody. (**A**) 1 µM GST–p21 was incubated at 4°C with 100 µg S100 extract from 293 cells. Concentrations (µM) of peptide competitor are indicated at the top: p21C2 peptide (lanes 2 and 3) or negative control peptide CSH262 (lanes 4–7). (**B**) As (A) except the reaction was carried out at 37°C. Lane 1, one tenth input lysate; lane 2, bound to GST protein; lanes 3–9, bound to 1 µM GST–p21 protein. Competing peptides were none (lanes 1–3) or the indicated concentrations of p21C2 or negative control peptide CSH262.

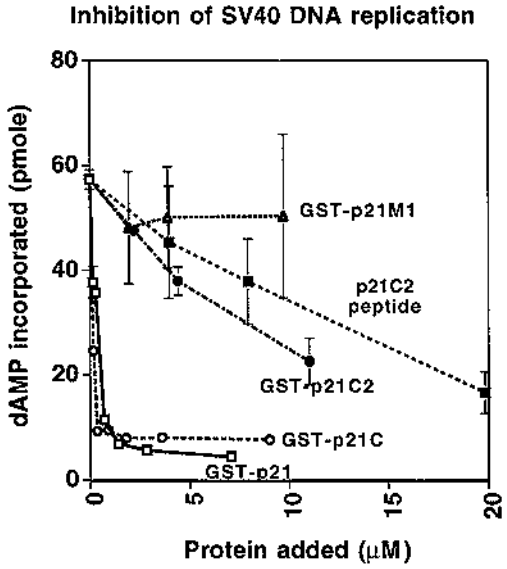

Figure 4. Inhibition of SV40 DNA replication by fragments of p21. The proteins added were GST–p21 (open squares), GST–p21C (open circles), GST–p21C2 (closed circles), GST–p21M1 (open triangles) and p21C2 peptide (closed squares). Each point represents the mean ± SD of three separate measurements of DNA replication (amount of dAMP incorporated into polynucleotide).

by stabilizing the p21–PCNA interaction. However, the 39 amino acid region of p21 was still an effective inhibitor of DNA replication *in vitro*.

Effect of GST–p21C and p21C2 peptides on entry of quiescent cells into S phase

To determine whether a p21-based peptide was active *in vivo* at reaching and interacting with PCNA we analyzed whether S phase was inhibited by these proteins. Quiescent diploid fibroblasts were stimulated by serum and entry into S phase followed after microinjection of GST fusion proteins or the p21C2 peptide (Fig. 5). GST–p21, GST–p21N and GST–p21C inhibited uptake of BrdU significantly compared with a negative control peptide CSH119, GST alone or GST fused to the cell cycle regulatory protein cdc25C (31). Thus GST–p21C inhibits growth of cells almost as well as GST–p21N when provided in high enough concentrations. Consistent with the result from the *in vitro* SV40 replication reaction, GST–p21C2 inhibited entry into S phase, although less effectively than GST–p21C. Surprisingly, the p21C2 peptide was only a weak inhibitor of cell growth. The difference between GST–p21C2 and the p21C2 peptide was observed consistently and was statistically significant ($P < 0.05$ by ANOVA). The results also confirm earlier reports that p21N, which binds and inhibits cdk kinases but not PCNA, inhibits growth of cells almost as effectively as p21.

Deletion mapping the part of PCNA which binds p21

Full-length PCNA and various deletion derivatives were synthesized by *in vitro* transcription–translation and binding to GST–p21 measured in a pull-down assay (Fig. 6). Since full-length PCNA bound to p21 well but a fragment of PCNA containing residues 40 to the C-terminus (40–C) did not, it appeared that the N-terminal portion of PCNA was important for binding p21. Consistent with this possibility, derivatives of PCNA containing amino acids 1–127 and 1–67 bound to p21. We conclude that a p21 binding domain of PCNA resides in the N-terminal 67 amino acids, perhaps even in the N-terminal 40 residues. The 1–127 fragment could have interacted with p21 indirectly as part of a larger complex with a protein present in the reticulocyte lysate (e.g. full-length rabbit PCNA). To test if this was the case the *in vitro* translation mix was fractionated by glycerol gradient sedimentation. The 'light' fractions, where the 1–127 fragment sediments in the same position as cytochrome c (and much lighter than the position of endogenous PCNA), could still associate with p21 (data not shown). Therefore, it is likely that the isolated 1–127 fragment of PCNA associates directly with p21.

The stoichiometry of the p21–PCNA interaction has been reported as 1:1 (p21 to trimer) (16) or 2.3:1 (18). Our observation that an isolated part of a PCNA monomer binds to p21 suggests that there could be more than one p21 binding site per PCNA trimer. p21C2 peptide was mixed with PCNA trimers at different ratios and subjected to gel filtration (Fig. 7). Even when p21C2 peptide was added at a ratio of 6 molecules peptide/PCNA trimer all the peptide was bound to PCNA and co-eluted with alcohol dehydrogenase (150 kDa). As a negative control p21C2 was mixed with another DNA replication/repair factor, Fen1, and subjected to gel filtration. All of the peptide eluted from the column after cytochrome c (14 kDa). The position of elution indicates that the p21C2 peptide is not present as a hexamer (30 kDa). Glycerol gradient sedimentation of 6-histidine-tagged p21 also indicates that the molecule exists as a monomer (16). Therefore, the association of virtually all the p21C2 peptide with PCNA even at a ratio of 6 peptide molecules/PCNA trimer is consistent with the model that there are multiple p21 binding sites per PCNA trimer (18). Even though there may be six potential binding sites for p21C2 peptide per PCNA trimer we favor a model where three molecules of p21 bind per PCNA trimer (see Discussion).

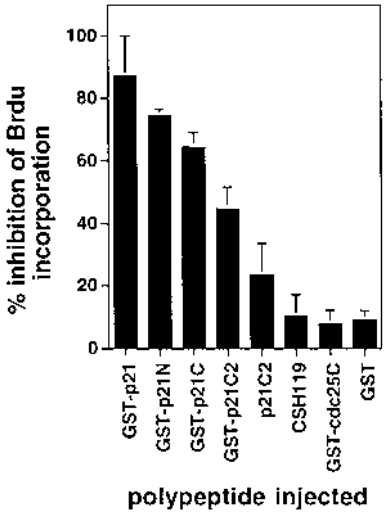

Figure 5. Inhibition of entry into S phase by microinjection of GST–p21 fusion proteins and indicated peptides into nuclei of serum re-activated diploid fibroblasts 15 h after re-activation. Mean ± SD for at least three different experiments are shown. CSH119, GST and GST–CDC25C were the negative controls, with indicated growth inhibition probably being a side effect of the injection procedure.

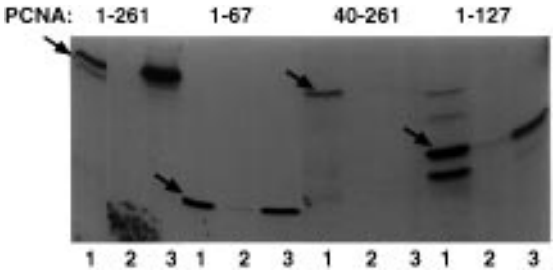

Figure 6. Deletion mapping of the part of PCNA that binds to p21. Full-length (1–261) or fragments containing the indicated residues of PCNA were produced by *in vitro* transcription–translation and visualized by fluorography. Lane 1, one tenth input; lane 2, protein bound to GST-coated beads; lane 3, protein bound to GST–p21-coated beads. Arrows indicate the PCNA (full-length or deletion derivative) in the input lane of each set.

Secondary structure of p21C2 peptide by circular dichroism and nuclear magnetic resonance

In view of the high affinity with which GST–p21C2 binds PCNA and inhibits S phase *in vivo*, a structural analog of the p21C2 domain would be a strong candidate for pharmacological use. Since the p21C2 peptide bound PCNA well at 4°C, we attempted to determine its structure.

The structure of the synthetic peptide p21C2 was studied by circular dichroism. A representative spectrum is shown in Figure 8. The peptide does not appear to have a well-defined secondary structure. The spectrum displays a minimum at 200 nm and a maximum at 220 nm (32). Temperature dependence of the CD spectra was monitored at 200 and 220 nm (Fig. 8, inset) and failed to show any appreciable change in ellipticity with change in temperature, confirming the lack of folded structure.

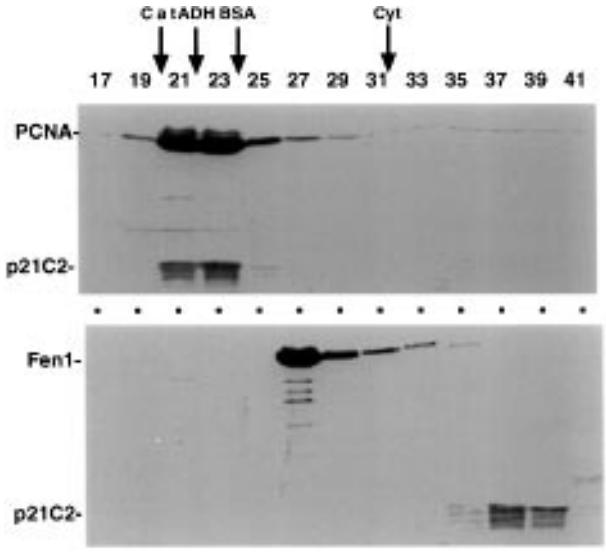

Figure 7. Gel filtration analysis of complexes formed by p21C2 peptide with PCNA (top) and Fen1 (bottom). Peptide and PCNA (molar ratio 2:1, equal to 6 molecules peptide/PCNA trimer) or peptide and Fen1 (molar ratio 2:1) were incubated and the complexes analyzed by chromatography on a Superose12 column. Alternate fractions were visualized by SDS–PAGE and Coomasie blue staining. The positions of elution of molecular weight markers is indicated by arrows at the top: catalase (Cat, 240 kDa), alcohol dehydrogenase (ADH, 150 kDa), bovine serum albumin (BSA, 66 kDa) and cytochrome c (Cyt, 12.5 kDa).

To further investigate the structure of the peptide ^{1}H NMR experiments were run in aqueous conditions. The NOESY spectrum (Fig. 9) lacks any significant number of inter-residue cross-peaks. The only cross-peaks seen are intra-residue, between amide protons and α protons (Fig. 9c) or side chain protons (Fig. 9d) of the same residue or sequentially adjacent residues. In particular, amide–amide cross-peaks are absent, which would be characteristic of an organized protein structure (Fig. 9a). Furthermore, the chemical shift values of each amino acid determined by TOCSY experiments are identical (within experimental error) to published random coil ^{1}H chemical shift values (data not shown) (33).

Altogether, the above spectroscopy results (circular dichroism and NMR), which did not vary under a large variety of aqueous conditions (temperature, buffer and pH; data not shown), demonstrate that unbound p21C2 does not adopt a well-defined structure in an aqueous environment.

DISCUSSION

The DNA replication enzymes are attractive targets for development of new agents for chemotherapy (34). We examined the p21–PCNA interaction with the long-term goal of determining if it could be exploited for the design of drugs which reach their target (PCNA) *in vivo*. As a first approximation we used a peptide (p21C2) derived from p21 which interacted with PCNA and inhibited the SV40 replication reaction *in vitro*. A 10-fold higher concentration of GST–p21C2 or the free p21C2 peptide was required to inhibit the SV40 replication reaction compared with GST–p21C. This is likely to be due to the 100-fold decrease in affinity of p21C2 for PCNA at physiological temperatures, although we cannot rule out the existence of factors in cell extracts that specifically interfere with the action of p21C2, but not p21C.

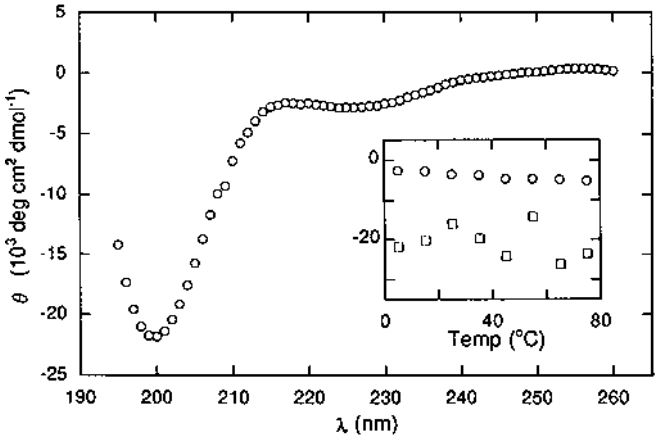

Figure 8. Far-UV circular dichroism spectrum of the p21C2 peptide in PBS (pH 7) at 4°C. (Inset) Effect of temperature on ellipticity measured at 220 nm (squares) and 200 nm (circles).

These results agree with a recent report that a 20 amino acid peptide from the C-terminal part of p21 (141–160) binds and inhibits PCNA *in vitro* (35). Point mutations have also indicated that multiple amino acids in this same region of p21 and additional ones at residues 161–163 are crucial for interaction with PCNA (36).

The efficacy of p21-based peptides at reaching and inhibiting PCNA *in vivo* was not clear before the present study. Because GST–p21C2 effectively inhibited cell growth but the free p21C2 peptide did not, we suspect that smaller peptides are unlikely to be useful in inhibiting PCNA *in vivo*. However, the high affinity of the interaction between GST–p21C and PCNA (K_d 10–20 nM) suggests that this interaction is suitable for pharmacological purposes. For comparison, other protein–protein interactions which have the potential for development as therapeutic agents include inhibition of cyclin–cdk kinases by p21 (K_i 1 nM) (37), interaction between phosphotyrosine-containing peptides and SH2 domains (K_d 10–100 nM) (38,39) and interaction between SH3 domains and proline-rich peptides (K_d 1000 nM) (40).

In general, peptide-based therapeutic agents suffer from the obvious problem of delivering peptides into cells at high concentrations. Our results point to two additional drawbacks: decreasing the length of the interacting peptide rendered the interaction thermodynamically unstable and additional poorly understood mechanisms were responsible for the small p21C2 peptide, but not GST–p21C2 protein, being inactivated in the cell. A small chemical that can mimic the structure of the active PCNA binding region of p21C2 may overcome all these drawbacks. Such a chemical may also be used to target other replication inhibitors to the site of DNA synthesis. Therefore, the best approach will be to determine the structure of the p21C2 binding interface and design chemicals which mimic this. Results reported in this paper indicate that the free p21C2 peptide lacks organized structure, suggesting that one has to determine the structure of the PCNA-bound peptide for this purpose.

Differences in the relative intracellular concentrations of p21C probably explain why S phase is inhibited by microinjection of GST–p21C, while transfection of plasmids expressing p21C failed to inhibit colony formation in an earlier assay (23,24). Expression from transfected plasmids is unlikely to yield as high a concentration of p21C per nucleus as is obtained by microinjection. Quiescent diploid fibroblasts have very little PCNA and as they enter the cell

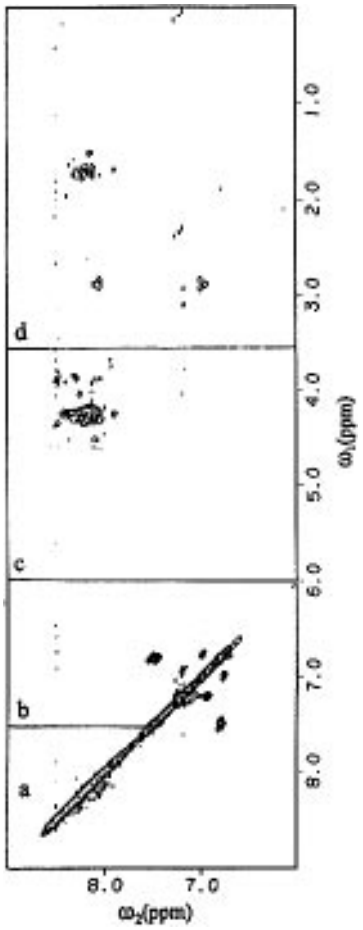

Figure 9. ^{1}H NOESY spectrum of p21C2 peptide in PBS at 25°C with a 150 ms mixing time. The low field half (ω_2 6.0–9.0 p.p.m.) of the spectrum is shown. Above the diagonal the spectrum is divided into four regions (a–d) where cross-peaks between distinct proton types occur (see text).

cycle new PCNA has to be synthesized to support DNA replication. Therefore, the low levels of PCNA and the fact that new PCNA is not sequestered in replication complexes are additional factors which favor cell growth suppression by p21C in the experiments reported here.

Using the two-hybrid method of studying protein–protein interactions another group has studied the domain of PCNA that interacts with p21 (35). A series of progressively increasing N-terminal deletions showed that amino acids 50–261 (50-C-terminus) and 100–261 of PCNA could interact with p21, but amino acids 150–261 could not, suggesting the importance of amino acids 100–150 of PCNA in the interaction with p21. Our biochemical method of assaying p21–PCNA interaction fails to show an interaction with the 40–261 derivative of PCNA, yet shows significant interaction of amino acids 1–67 or 1–127 of PCNA with p21. The two-hybrid method uses a version of PCNA with the yeast Gal4 activation domain fused at the N-terminus. Such a fusion may partially denature PCNA and permit interactions not possible with the trimeric PCNA complex. We find that GST–PCNA (where GST protein is fused to the N-terminus of PCNA) does not bind p21 (data not shown), so that the Gal4–PCNA fusion may also have inactivated the N-terminal p21 binding site. Alternatively, each PCNA molecule being composed of two structurally homologous

domains, amino acids 1–67 and 100–150 contain structurally similar N-terminal regions from each of the two domains (41). Therefore, the interaction with p21 could be executed by two structurally homologous regions of PCNA: a strong p21 binding region at the N-terminus and a weak binding region at amino acids 100–150. The weaker binding site in the 40–261 derivative may not be sufficient to give a positive signal in our assay, but could give a signal in the more sensitive two-hybrid assay. If this alternative is correct, each PCNA trimer may have up to six potential binding sites for p21.

The flexible nature of the p21C2 peptide may have been created by deletion of more than 75% of the p21 protein. However, despite the flexible structure, the high affinity and specificity of GST–p21C2 for PCNA at 4°C suggests that p21C2 is induced into a specific conformation when interacting with PCNA. This possibility is also favored by the observation that interaction of the 39 amino acid region is temperature sensitive and that the adjoining 38 amino acids stabilize the interaction (GST–p21C2 versus GST–p21C at 37°C).

Since isolated PCNA monomers and portions thereof bind p21, there are likely to be more than one p21 binding site per PCNA trimer. Are there six binding sites per PCNA trimer? We have provided experimental evidence which suggest that six p21C2 peptides could bind per PCNA trimer. However, it is unlikely that six molecules of p21 could bind to PCNA and not change the sedimentation profile of PCNA (16). Surface plasmon resonance spectroscopy showed that 2.3 molecules of p21 bind per PCNA trimer (18). Therefore, although there may be six sites per PCNA ring for association with p21, only a fraction of these can be occupied simultaneously by a molecule as large as p21. Nevertheless, multiple p21C2 binding sites on each PCNA ring translate into multiple binding sites for a chemical based on the binding interface of the peptide.

In conclusion, these results indicate that the p21–PCNA interaction has properties that may be useful for the design of drugs targeted to the replication fork. The affinity of the interaction is high, as are the number of binding sites per PCNA trimer. GST fusion proteins containing the peptide can interact with PCNA in the cell. However, direct use of peptides based on p21 will not be useful. Instead, one will have to determine the structure of the binding interface of p21 in the p21–PCNA complex and design chemicals based on this structure.

ACKNOWLEDGEMENTS

We thank members of the Dutta Laboratory and G.Lindenmeyer and D.Gilbert for helpful discussions, J.Morrow for technical assistance, J.Parvin for reading the manuscript, C.Dahl for help with peptide synthesis and J.Lee for use of the CD spectrometer. This work was supported by a grant from the NIH (CA60499) and career development awards from the American Cancer Society (JFRA 474) and the US Armed Forces Medical Research Command (DAMD17-94-J-4064). JC was supported by a post-doctoral fellowship (DAMD 17-94-J-4070), RP is a Howard Hughes Medical Institute Physician Post-doctoral Fellow, and MP was supported in part by HSFP grant RG-496/93.

REFERENCES

1 Xiong,Y., Zhang,H. and Beach,D. (1992) *Cell*, **71**, 505–514.
2 Zhang,H., Xiong,Y. and Beach,D. (1993) *Mol. Biol. Cell*, **4**, 897–906.
3 Xiong,Y., Zhang,H. and Beach,D. (1993) *Genes Dev.*, **7**, 1572–1583.
4 Xiong,Y., Hannon,G.J., Zhang,H., Casso,D., Kobayashi,R. and Beach,D. (1993) *Nature*, **366**, 701–704.
5 Harper,J.W., Adami,G.R., Wei,N., Keyomarsi,K. and Elledge,S.J. (1993) *Cell*, **75**, 805–816.
6 el Deiry,W.S., Tokino,T., Velculescu,V.E., Levy,D.B.,Parsons,R., Trent,J.M., Lin,D., Mercer,W.E., Kinzler,K.W. and Vogelstein,B. (1993) *Cell*, **75**, 817–825.
7 Gu,Y., Turck,C.W. and Morgan,D.O. (1993) *Nature*, **366**, 707–710.
8 Noda,A., Ning,Y., Venable,S.F., Pereira,S.O. and Smith,J.R. (1994) *Exp. Cell Res.*, **211**, 90–98.
9 Prelich,G., Tan,C.K., Kostura,M., Mathews,M.B., So,A.G., Downey,K.M. and Stillman,B. (1987) *Nature*, **326**, 517–520.
10 Prelich,G., Kostura,M., Marshak,D.R., Mathews,M.B. and Stillman,B. (1987) *Nature*, **326**, 471–475.
11 Prelich,G. and Stillman,B. (1988) *Cell*, **53**, 117–126.
12 Lee,M.Y., Jiang,Y.Q., Zhang,S.J. and Toomey,N.L. (1991) *J. Biol. Chem.*, **266**, 2423–2429.
13 Weiser,T., Gassmann,M., Thommes,P., Ferrari,E., Hafkemeyer,P. and Hubscher,U. (1991) *J. Biol. Chem.*, **266**, 10420–10428.
14 Podust,L.M., Podust,V.N., Floth,C. and Hubscher,U. (1994) *Nucleic Acids Res.*, **22**, 2970–2975.
15 Maga,G. and Hubscher,U. (1995) *Biochemistry*, **34**, 891–901.
16 Waga,S., Hannon,G.J., Beach,D. and Stillman,B. (1994) *Nature*, **369**, 574–578.
17 Li,R., Waga,S., Hannon,G.J., Beach,D. and Stillman,B. (1994) *Nature*, **371**, 534–537.
18 Flores-Rozas,H., Kelman,Z., Dean,F.B., Pan,Z.-Q., Harper,J.W., Elledge,S.J., O'Donnell,M. and Hurwitz,J. (1994) *Proc. Natl. Acad. Sci. USA*, **91**, 8655–8659.
19 Strausfeld,U.P., Howell,M., Rempel,R., Maller,J.L., Hunt,T. and Blow,J.J. (1994) *Curr. Biol.*, **4**, 876–883.
20 Shivji,M., Grey,S.J., Strausfeld,U.P., Wood,R.D. and Blow,J.J. (1994) *Curr. Biol.*, **4**, 1062–1068.
21 Podust,V.N., Podust,L.M., Goubin,F., Ducommun,B. and Hubscher,U. (1995) *Biochemistry*, **34**, 8869–8875.
22 el Deiry,W.S., Harper,J.W., O'Connor,P.M., Velculescu,V.E., Canman,C.E., Jackman,J., Pietenpol,J.A., Burrell,M., Hill,D.E., Wang,Y.S. *et al.* (1994) *Cancer Res.*, **54**, 1169–1174.
23 Chen,J., Jackson,P.K., Kirschner,M.W. and Dutta,A. (1995) *Nature*, **374**, 386–388.
24 Nakanishi,M., Robetorye,R.S., Adami,G.R., Pereirasmith,O.M. and Smith,J.R. (1995) *EMBO J.*, **14**, 555–563.
25 Luo,Y., Hurwitz,J. and Massague,J. (1995) *Nature*, **375**, 159–161.
26 Fien,K. and Stillman,B. (1992) *Mol. Cell. Biol.*, **12**, 155–163.
27 Dutta,A., Ruppert,J.M., Aster,J.C. and Winchester,E. (1993) *Nature*, **365**, 79–82.
28 Dutta,A. and Stillman,B. (1992) *EMBO J.*, **11**, 2189–2199.
29 Scatchard,G. (1949) *Annls NY Acad. Sci.*, **51**, 660–684.
30 Pepperkok,R. (1995) In Pagano,M. (ed.), *Cell Cycle: Materials and Methods*. Springer-Verlag, Heidelberg, Germany, pp. 75–86.
31 Hoffmann,I., Draetta,G. and Karsenti,E. (1994) *EMBO J.*, **13**, 4302–4310.
32 Johnson,W.C. (1990) *Proteins Struct. Functions Genet.*, **7**, 205–214.
33 Wuthrich,K. (1986) In *NMR of Proteins and Nucleic Acids*. John Wiley & Sons, Chichester, UK, p. 17.
34 Hubscher,U. and Spadari,S. (1994) *Physiol. Rev.*, **74**, 259–304.
35 Warbrick,E., Lane,D.P., Glover,D.M. and Cox,L.S. (1995) *Curr. Biol.*, **5**, 275–282.
36 Goubin,F. and Ducommun,B. (1995) *Oncogene*, **10**, 2281–2287.
37 Harper,J.W., Elledge,S.J., Keyomarsi,K., Dynlacht,B., Tsai,L.H., Zhang,P., Dobrowolski,S., Bai,C., Connell-Crowley,L., Swindell,E. *et al.* (1995) *Mol. Biol. Cell*, **6**, 387–400.
38 Songyang,Z., Shoelson,S.E., Chaudhuri,M., Gish,G., Pawson,T., Haser,W.G., King,F., Roberts,T., Ratnofsky,S., Lechleider,R.J. *et al.* (1993) *Cell*, **72**, 767–778.
39 Panayotou,G., Gish,G., End,P., Truong,O., Gout,I., Dhand,R., Fry,M.J., Hiles,I., Pawson,T. and Waterfield,M.D. (1993) *Mol. Cell. Biol.*, **13**, 3567–3576.
40 Yu,H., Chen,J.K., Feng,S., Dalgarno,D.C., Brauer,A.W. and Schreiber,S.L. (1994) *Cell*, **76**, 933–945.
41 Krishna,T.S., Kong,X.P., Gary,S., Burgers,P.M. and Kuriyan,J. (1994) *Cell*, **79**, 1233–1243.